Testing Lorentz Invariance and CPT Conservation with NuMI Neutrinos in the MINOS Near Detector

P. Adamson,[9] C. Andreopoulos,[19] K. E. Arms,[15] R. Armstrong,[12] D. J. Auty,[23] D. S. Ayres,[1] B. Baller,[9] G. Barr,[17] W. L. Barrett,[28] B. R. Becker,[15] A. Belias,[19] R. H. Bernstein,[9] D. Bhattacharya,[18] M. Bishai,[4] A. Blake,[6] G. J. Bock,[9] J. Boehm,[10] D. J. Boehnlein,[9] D. Bogert,[9] C. Bower,[12] E. Buckley-Geer,[9] S. Cavanaugh,[10] J. D. Chapman,[6] D. Cherdack,[26] S. Childress,[9] B. C. Choudhary,[9] S. J. Coleman,[29] A. J. Culling,[6] J. K. de Jong,[11] M. V. Diwan,[4] M. Dorman,[14,19] S. A. Dytman,[18] C. O. Escobar,[7] J. J. Evans,[14,17] E. Falk Harris,[23] G. J. Feldman,[10] M. V. Frohne,[3] H. R. Gallagher,[26] M. C. Goodman,[1] P. Gouffon,[20] R. Gran,[16] E. W. Grashorn,[15] N. Grossman,[9] K. Grzelak,[27,17] A. Habig,[16] D. Harris,[9] P. G. Harris,[23] J. Hartnell,[23,19] R. Hatcher,[9] K. Heller,[15] A. Himmel,[5] A. Holin,[14] J. Hylen,[9] G. M. Irwin,[22] M. Ishitsuka,[12] D. E. Jaffe,[4] C. James,[9] D. Jensen,[9] T. Kafka,[26] S. M. S. Kasahara,[15] J. J. Kim,[21] G. Koizumi,[9] S. Kopp,[25] M. Kordosky,[29,14] D. J. Koskinen,[14] A. Kreymer,[9] S. Kumaratunga,[15] K. Lang,[25] J. Ling,[21] P. J. Litchfield,[15] R. P. Litchfield,[17] L. Loiacono,[25] P. Lucas,[9] J. Ma,[25] W. A. Mann,[26] M. L. Marshak,[15] J. S. Marshall,[6] N. Mayer,[12] A. M. McGowan,[1,15] J. R. Meier,[15] M. D. Messier,[12] C. J. Metelko,[19] D. G. Michael,[5,*] J. L. Miller,[13,*] W. H. Miller,[15] S. R. Mishra,[21] C. D. Moore,[9] J. Morfín,[9] L. Mualem,[5] S. Mufson,[12] S. Murgia,[22] J. Musser,[12] D. Naples,[18] J. K. Nelson,[29] H. B. Newman,[5] R. J. Nichol,[14] T. C. Nicholls,[19] J. P. Ochoa-Ricoux,[5] W. P. Oliver,[26] R. Ospanov,[25] J. Paley,[12] V. Paolone,[18] A. Para,[9] T. Patzak,[8] Ž. Pavlović,[25] G. Pawloski,[22] G. F. Pearce,[19] C. W. Peck,[5] D. A. Petyt,[15] R. Pittam,[17] R. K. Plunkett,[9] A. Rahaman,[21] R. A. Rameika,[9] T. M. Raufer,[19] B. Rebel,[9] J. Reichenbacher,[1] P. A. Rodrigues,[17] C. Rosenfeld,[21] H. A. Rubin,[11] M. C. Sanchez,[1,10] N. Saoulidou,[9] J. Schneps,[26] P. Schreiner,[3] P. Shanahan,[9] W. Smart,[9] A. Sousa,[17] B. Speakman,[15] P. Stamoulis,[2] M. Strait,[15] N. Tagg,[26] R. L. Talaga,[1] M. A. Tavera,[23] J. Thomas,[14] J. Thompson,[18,*] M. A. Thomson,[6] J. L. Thron,[1] G. Tinti,[17] G. Tzanakos,[2] J. Urheim,[12] P. Vahle,[29,14] B. Viren,[4] M. Watabe,[24] A. Weber,[17] R. C. Webb,[24] A. Wehmann,[9] N. West,[17] C. White,[11] S. G. Wojcicki,[22] T. Yang,[22] M. Zois,[2] K. Zhang,[4] and R. Zwaska[9]

(MINOS Collaboration)

[1]*Argonne National Laboratory, Argonne, Illinois 60439, USA*
[2]*Department of Physics, University of Athens, GR-15771 Athens, Greece*
[3]*Physics Department, Benedictine University, Lisle, Illinois 60532, USA*
[4]*Brookhaven National Laboratory, Upton, New York 11973, USA*
[5]*Lauritsen Laboratory, California Institute of Technology, Pasadena, California 91125, USA*
[6]*Cavendish Laboratory, University of Cambridge, Madingley Road, Cambridge CB3 0HE, United Kingdom*
[7]*Universidade Estadual de Campinas, IF-UNICAMP, CP 6165, 13083-970, Campinas, SP, Brazil*
[8]*APC-Université Paris 7 Denis Diderot, 10, rue Alice Domon et Léonie Duquet, F-75205 Paris Cedex 13, France*
[9]*Fermi National Accelerator Laboratory, Batavia, Illinois 60510, USA*
[10]*Department of Physics, Harvard University, Cambridge, Massachusetts 02138, USA*
[11]*Physics Division, Illinois Institute of Technology, Chicago, Illinois 60616, USA*
[12]*Indiana University, Bloomington, Indiana 47405, USA*
[13]*Physics Department, James Madison University, Harrisonburg, Virginia 22807, USA*
[14]*Department of Physics and Astronomy, University College London, Gower Street, London WC1E 6BT, United Kingdom*
[15]*University of Minnesota, Minneapolis, Minnesota 55455, USA*
[16]*Department of Physics, University of Minnesota-Duluth, Duluth, Minnesota 55812, USA*
[17]*Subdepartment of Particle Physics, University of Oxford, Oxford OX1 3RH, United Kingdom*
[18]*Department of Physics and Astronomy, University of Pittsburgh, Pittsburgh, Pennsylvania 15260, USA*
[19]*Rutherford Appleton Laboratory, Chilton, Didcot, Oxfordshire, OX11 0QX, United Kingdom*
[20]*Instituto de Física, Universidade de São Paulo, CP 66318, 05315-970, São Paulo, SP, Brazil*
[21]*Department of Physics and Astronomy, University of South Carolina, Columbia, South Carolina 29208, USA*
[22]*Department of Physics, Stanford University, Stanford, California 94305, USA*
[23]*Department of Physics and Astronomy, University of Sussex, Falmer, Brighton BN1 9QH, United Kingdom*
[24]*Physics Department, Texas A&M University, College Station, Texas 77843, USA*
[25]*Department of Physics, University of Texas at Austin, 1 University Station C1600, Austin, Texas 78712, USA*
[26]*Physics Department, Tufts University, Medford, Massachusetts 02155, USA*
[27]*Department of Physics, Warsaw University, Hoa 69, PL-00-681 Warsaw, Poland*
[28]*Physics Department, Western Washington University, Bellingham, Washington 98225, USA*
[29]*Department of Physics, College of William & Mary, Williamsburg, Virginia 23187, USA*
(Received 1 July 2008; published 9 October 2008)

A search for a sidereal modulation in the MINOS near detector neutrino data was performed. If present, this signature could be a consequence of Lorentz and *CPT* violation as predicted by the effective field theory called the standard-model extension. No evidence for a sidereal signal in the data set was found, implying that there is no significant change in neutrino propagation that depends on the direction of the neutrino beam in a sun-centered inertial frame. Upper limits on the magnitudes of the Lorentz and *CPT* violating terms in the standard-model extension lie between 10^{-4} and 10^{-2} of the maximum expected, assuming a suppression of these signatures by a factor of 10^{-17}.

DOI: 10.1103/PhysRevLett.101.151601 PACS numbers: 11.30.Cp, 11.30.Er, 14.60.Pq

At experimentally accessible energies, signals for Lorentz and *CPT* violation can be described by a theory based on the standard model and general relativity, referred to as the standard-model extension (SME) [1,2]. The SME was developed following the suggestion in string theory that extended quantum strings introduce nonlocality that could break Lorentz invariance [3]. It is an observer-independent theoretical framework that contains all the Lorentz-violating (LV) terms involving particle fields in the standard model of particle physics and gravitational fields in general relativity (GR). SME is an effective field theory with quantum field action applying to quantum fields and elementary particles and classical action applying to gravitational fields. Since the standard model is thought to be the low-energy limit of a more fundamental theory that unifies quantum physics and gravity at the Planck scale, $m_P \simeq 10^{19}$ GeV, it has been suggested [2] that the violations of Lorentz and *CPT* symmetries introduced by SME provide a link to Planck scale physics. Although the magnitude of LV signatures in the accessible energy limit are suppressed by a factor of order the electroweak scale divided by the Planck scale, $m_W/m_P \sim 10^{-17}$ [4], these low-energy probes of new physics can and have been explored in many ways with current experimental technologies [5].

The SME framework predicts several unconventional phenomena, among which is one that arises from the dependence of the neutrino oscillation probability on the direction of neutrino propagation [4]. For experiments like MINOS [6] with both beam neutrino source and detector fixed on Earth's surface, Earth's sidereal rotation causes the direction of neutrino propagation $\hat{p}$ to change with respect to the Sun-centered inertial frame in which the SME is formulated [7]. The theory predicts that this rotation introduces a sidereal variation in the number of neutrinos detected from the beam. The LSND collaboration [7] did not see this signal. In this paper we use a sample of neutrinos identified in the MINOS near detector (ND) in a search for this sidereal signal. The neutrinos were generated by the Neutrinos at the Main Injector (NuMI) neutrino beam at Fermilab [8], whose flavor composition is 98.7% $\nu_\mu + \bar{\nu}_\mu$ [6].

According to the SME, the probability that one of these ν_μ oscillates to flavor ν_x, where x is e or τ, over a distance L from its production to detection due to Lorentz and *CPT* violation is given by [4]

$$P_{\nu_\mu \to \nu_x} \simeq L^2[(\mathcal{C})_{\mu x} + (\mathcal{A}_c)_{\mu x}\cos(\omega_\oplus T_\oplus) + (\mathcal{A}_s)_{\mu x}\sin(\omega_\oplus T_\oplus) + (\mathcal{B}_c)_{\mu x}\cos(2\omega_\oplus T_\oplus) + (\mathcal{B}_s)_{\mu x}\sin(2\omega_\oplus T_\oplus)]^2, \quad (1)$$

where $\omega_\oplus = 2\pi/(23^h 56^m 04.0982^s)$ is the Earth's sidereal frequency and $T_\oplus$ is the local sidereal time of the neutrino detection. For the MINOS ND, $\langle L \rangle \sim 750$ m. In this equation, the expressions for $(\mathcal{A}_c)_{\mu x}$, $(\mathcal{A}_s)_{\mu x}$, and $(\mathcal{C})_{\mu x}$ include both *CPT* and Lorentz-violating terms; the expressions for $(\mathcal{B}_c)_{\mu x}$ and $(\mathcal{B}_s)_{\mu x}$ include only Lorentz-violating terms. Since *CPT* violation implies Lorentz violation in field theory [9], there are no terms that depend on *CPT* violation alone. These parameters are combinations of the SME coefficients $(a_L)^\mu$ and $(c_L)^{\mu\nu}$ that describe LV [4]. The magnitude of the coefficients in Eq. (1) also depend on the neutrino propagation direction. For the NuMI beam line, the direction vectors of the beam are defined by colatitude $\chi = (90° - \text{latitude}) = 90.° - 41.840\,563\,33°$, $\theta = 93.346°$, and $\phi = 23.909°$. Here θ and ϕ are the beam zenith and azimuthal angles; θ is measured from the z axis which points toward the zenith; ϕ is defined from the x axis which is along the detector axis and increases away from the NuMI target. The y axis makes a right-handed coordinate system. The explicit relationships between the SME coefficients and the beam direction are found in [4]. In Eq. (1), the *CPT* violating terms depend on L and the Lorentz-violating terms depend on $L \times E_\nu$, where E_ν is the neutrino energy. This unconventional behavior arises because the SME is a perturbation theory in which the expansion is in powers of the derivative of the field, and is to be compared with the L/E_ν dependence of the oscillation probability resulting from nonzero neutrino masses [10]. The expansion introduces a factor of E_ν into the coefficients for each derivative, which results in this behavior.

The MINOS ND [11] is a magnetized 0.98 kton steel scintillator tracking calorimeter that lies 103 m underground at Fermilab and it is made of 282 octagonal planes, each having an area of 4×6 m^2. Each plane is comprised of a 2.54 cm thick steel plate and a layer of scintillator strips with dimensions of 4.1 cm $\times$ 1 cm. Each scintillator strip is coupled via wavelength-shifting fiber to one pixel of a 64-pixel Hamamatsu M64 PMT [12]. The ND readout

continuously integrates the PMT charges, while the data acquisition accepts data above a threshold of 0.25 photoelectrons.

Protons with mean energy of 120 GeV/c are extracted from the Main Injector in a beam spill of 10 μs duration. Spills are spaced by a period of approximately 2.4 s. The number of protons delivered to the target for each spill (POT) was measured using toroidal beam current transformers. The uncertainty in the number of POT for each spill is $\pm 1.0\%$ [6]. Neutrino events in the ND fiducial volume were selected based on their timing and spatial information [8,13]. The neutrinos were separated into charged currentlike (CC) or neutral currentlike (NC) events, as described in [8]. CC ν_μ events, identified by a μ^- track [6], were selected for further analysis to maximize the $\nu_\mu \rightarrow \nu_x$ oscillation signal in MINOS.

Standard beam quality cuts [6] were applied to select spills for the analysis. In addition, data quality cuts were applied to remove runs in which there were detector problems, including cooling system failures, magnetic coil failures, or an incorrectly configured readout trigger.

The data were taken during two run periods. The parameters for these two runs are given in Table I. The numbers of events and POT given are the numbers remaining in the sample after all cuts have been made.

Since the local sidereal phase histograms in this analysis require accurate event timing, we describe how time stamps are generated. The spill time is determined by the global positioning system (GPS) receiver located in the ND hall that reads out absolute universal coordinated time (UTC) and is accurate to 200 ns [14]. The main injector accelerates protons to 120 GeV/c and the spills are extracted to NuMI using a pulsed dipole magnet. The GPS time of the extraction magnet signal is recorded and defines the spill time [14].

Each neutrino event was tagged with the local sidereal time (LST) of its spill—the GPS spill time converted to sidereal time. The local sidereal phase of an event is given by LST $\times$ ($\omega_\oplus/2\pi$) and has a range of 0–1. Event times were not corrected for their time within a spill, an approximation that introduces no significant systematic error into the analysis.

The events in each spill were placed into a single bin in a histogram spanning 0–1 in local sidereal phase (LSP). The POT in the spill were binned into a second LSP histogram. By dividing these two histograms, we get the number of ν_μ events/POT as a function of LSP. This final histogram gives the normalized neutrino event rate in which we search for sidereal variations.

We used 32 bins for the LSP histograms. This binning was chosen to search for sidereal variations with a Fast Fourier Transform (FFT) [15] and the algorithm works most efficiently for $2^{\mathcal{N}}$ bins. Since Eq. (1) puts power into harmonic frequencies associated with Fourier terms to $n\omega_\oplus$, and for this analysis $n = 1$–4, we chose $\mathcal{N} = 5$ as the minimal binning that retains these harmonic terms. Each bin spans 0.031 in LSP or 45 min in sidereal time. The histograms of the ν_μ events/POT as a function of LSP for run I and run II are given in Fig. 1. The differences in the average event rates in the two runs are due primarily to different relative positions of the target and magnetic focusing horns for the two runs.

We performed an FFT analysis on the run I and run II sidereal phase histograms in Fig. 1 and we computed the weighted mean of the powers returned for the even (cos) and odd (sin) powers for harmonic frequencies out to $4\omega_\oplus T_\oplus$. The weighting factors were the mean event rates for each run. The resulting mean powers, $\bar{p}$(FFT), are listed in Table II.

These results were tested for several possible systematic effects. We found that systematic increases or decreases in the event rate of 5% in 6 months do not affect these results. We also searched for systematic changes in the rates from day to night and found no variations $>0.1\%$. In addition, we searched and found no sidereal modulation in the CC/NC ratio for these data. These tests show that systematic effects associated with neutrino production do not affect this sidereal analysis.

We constructed 1000 simulated experiments for both runs without a sidereal signal to test the significance of the powers given in Table II. We used the data themselves to construct these experiments. We first generated 1000 sets of sidereal phases for run I and run II, with each set having the same number of entries as spills in the run. The

TABLE I. Run parameters.

	CC Events	POT	Run Dates
Run I	1.82×10^6	1.25×10^{20}	May05–Feb06
Run II	1.62×10^6	1.14×10^{20}	Sept06–Mar07

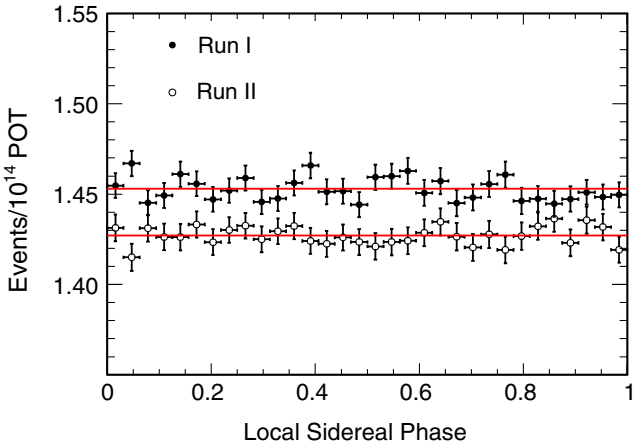

FIG. 1 (color online). The local sidereal phase histograms for run I and run II. Superposed are fits to a constant sidereal rate.

TABLE II. Weighted mean of run I and run II FFT powers in first four even/odd harmonic coefficients; $\mathcal{P}_F$ is the probability that the mean power is a noise fluctuation.

cos ()	$\bar{p}$(FFT)	$\mathcal{P}_F$	sin()	$\bar{p}$(FFT)	$\mathcal{P}_F$
$(\omega_\oplus T_\oplus)$	−0.002	0.91	$(\omega_\oplus T_\oplus)$	0.024	0.18
$(2\omega_\oplus T_\oplus)$	0.011	0.54	$(2\omega_\oplus T_\oplus)$	0.011	0.54
$(3\omega_\oplus T_\oplus)$	−0.006	0.74	$(3\omega_\oplus T_\oplus)$	-0.004	0.83
$(4\omega_\oplus T_\oplus)$	−0.016	0.37	$(4\omega_\oplus T_\oplus)$	0.023	0.20

phases were drawn randomly from the sidereal phase distribution constructed from the start times for each spill in the run I or run II data set. We then put the events for each spill in the run into 1000 separate histograms according to the scrambled sidereal phase assigned. The number of POT for that spill was entered into a second set of 1000 histograms according to the same set of sidereal phases. The division of each event histogram by its corresponding POT histogram results in the simulated experiments—histograms of the number of ν_μ events/POT as a function of LSP without a signal.

We performed the same FFT analysis on each of the 1000 run I and 1000 run II simulated experiments as was done with the sidereal phase histograms in Fig. 1. The powers returned by these FFTs give the fluctuation spectrum expected from sidereal phase histograms in which there is no sidereal signal. As for the data, we computed the weighted mean power for each harmonic in a pair of simulated run I and run II experiments. The distributions for the even (cos) and the odd (sin) mean powers for harmonic frequencies out to $4\omega_\oplus T_\oplus$ are shown superposed in Fig. 2. Clearly these even and odd distributions are nearly identical. In addition, a Gaussian of width $\sigma = 1.8 \times 10^{-2}$ has been superposed onto these two distributions in Fig. 2. This fit was obtained independently for both distributions. We use this Gaussian to estimate the probability that the powers returned by the FFT analysis of the sidereal phase histograms in Fig. 1 are due to statistical fluctuations.

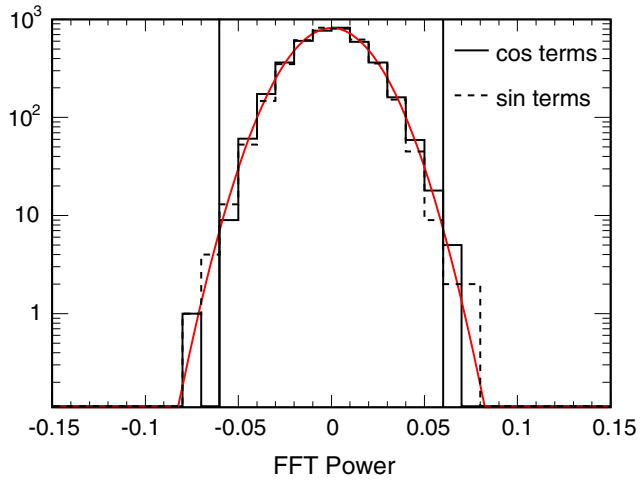

FIG. 2 (color online). The distributions for the even (cos) and the odd (sin) mean powers for harmonic frequencies to $4\omega_\oplus T_\oplus$ from the FFT analysis of 1000 simulated experiments in run I and run II. Superposed on these distributions is a Gaussian fit of width $\sigma = 1.8 \times 10^{-2}$. This fit was obtained independently for both distributions. Values outside of the vertical lines are more than 3σ from the mean.

Table II gives the probability, $\mathcal{P}_F$, that the mean power represents a noise fluctuation. It was calculated as the probability of drawing a value of the weighted mean power for the two data sets at least as large as found from the parent Gaussian distribution in Fig. 2. Since the largest fluctuation in the FFT power in the Fig. 1 histogram is 1.32σ we conclude that no term reaches the level of a 3σ detection. We have determined that these results are insensitive to the exact choice of the zero point of sidereal phase. This model-independent result implies that there is no significant change in normalized neutrino event rate that depends on the direction of the neutrino beam in a sun-centered inertial frame. In the context of SME, this result is inconsistent with the detection of LV.

In the absence of a sidereal signal, we can establish upper limits on the SME coefficients $(a_L)^\mu$ and $(c_L)^{\mu\nu}$ that describe LV [4] using the standard MINOS Monte Carlo simulation. The simulation includes weighting to account for hadron production off the NuMI target [6]. In this simulation, events are generated by modeling the NuMI beam line, including the hadron production by the 120 GeV/c protons on target, the propagation of the hadrons through the focusing elements and 675 m decay pipe to the beam absorber, and the calculation of the probability that any neutrinos generated traverse the ND. The ND neutrino event simulation takes the neutrinos from the NuMI simulation, along with an energy determined by decay kinematics, and uses this information as input into the simulation of the ND. With the known L and E_ν for the simulated neutrino events, as well as the beam direction, we can inject a Lorentz-violating signal into Eq. (1). The construction of MC-generated sidereal phase histograms is described elsewhere [16].

TABLE III. Limits to the magnitudes of the SME coefficients for $\nu_\mu \to \nu_x$ in terms of the suppression factor $m_W/m_P \sim 10^{-17}$; a_L have units of (GeV) and c_L are unitless.

	$\times 10^{-17}$		$\times 10^{-17}$
a_L^X	3.0×10^{-3}	a_L^Y	3.0×10^{-3}
c_L^{TX}	0.9×10^{-5}	c_L^{TY}	0.9×10^{-5}
c_L^{XX}	5.6×10^{-4}	c_L^{YY}	5.5×10^{-4}
c_L^{XY}	2.7×10^{-4}	c_L^{YZ}	1.2×10^{-4}
c_L^{XZ}	1.3×10^{-4}	...	...

The limits on the LV coefficients $(a_L)^\mu$ and $(c_L)^{\mu\nu}$ were determined from a set of 200 simulated experiments. First we set all but one LV coefficient to zero. We next weighted the simulated neutrino events in each histogram by its survival probability computed according to Eq. (1), assuming the LV coefficient is small. We then increased the magnitude of the nonzero coefficient until one of the FFT powers in the simulated phase histogram was 3σ away from the mean of the distribution in Fig. 2. An average of the 200 determinations of each SME coefficient, scaled in terms of the suppression factor $m_W/m_p \sim 10^{-17}$, is given in Table III. This procedure, by which we vary one parameter at a time to determine the limits, could miss fortuitous cancellations of SME coefficients thereby masking a signal. In these cases we can determine no limits to the LV coefficients.

In summary, we find no significant evidence for sidereal variations in the MINOS ND neutrino data. When framed in the SME theory [4], this result leads to the conclusion that we have detected no evidence for the violation of Lorentz and *CPT* invariance. Based on these results, we computed limits on the LV SME coefficients and find that their magnitude is $<1\%$ of the suppression factor $m_W/m_P \sim 10^{-17}$. For the a_L-type SME coefficients, the MINOS limits are a factor of 3 lower than those reported by LSND [7]; for the c_L-type SME coefficients, the MINOS limits are at least 4 orders of magnitude lower than LSND's. The improvement in the limits to the a_L-type coefficients, which depend on L^2, can be explained by the longer baseline to the MINOS near detector. The more significant improvement in the limits to the c_L-type coefficients, which depend on both the distance traveled by the neutrino and its energy as $(E_\nu \times L)^2$, can be explained by the longer baseline coupled with the more energetic MINOS neutrinos [4].

We gratefully acknowledge the many valuable conversations with Alan Kostelecký during the course of this work. This work was supported by the U.S. DOE, the UK STFC, the U.S. NSF, the State and University of Minnesota, the University of Athens, Greece, and Brazil's FAPESP and CNPq. We are grateful to the Minnesota Department of Natural Resources, the crew of the Soudan Underground Laboratory, and the staff of Fermilab for their contribution to this effort.

*Deceased.

[1] G. Amelino-Camelia *et al.*, AIP Conf. Proc. **758**, 30 (2005); R. Bluhm, Lect. Notes Phys. **702**, 191 (2006).

[2] D. Colladay and V. A. Kostelecký, Phys. Rev. D **55**, 6760 (1997); D. Colladay and V. A. Kostelecký, Phys. Rev. D **58**, 116002 (1998); V. A. Kostelecký, Phys. Rev. D **69**, 105009 (2004).

[3] V. A. Kostelecký and S. Samuel, Phys. Rev. D **39**, 683 (1989).

[4] V. A. Kostelecký and M. Mewes, Phys. Rev. D **70**, 076002 (2004).

[5] S. Reinhardt *et al.*, Nature Phys. **3**, 861 (2007); H. Muller *et al.*, Phys. Rev. Lett. **99**, 050401 (2007); V. W. Hughes *et al.*, Phys. Rev. Lett. **87**, 111804 (2001); Y. B. Hsiung *et al.*, Nucl. Phys. B, Proc. Suppl. **86**, 312 (2000); J. Link *et al.*, Phys. Lett. B **556**, 7 (2003); B. Aubert *et al.*, Phys. Rev. D **70**, 012007 (2004); J. B. R. Battat *et al.*, Phys. Rev. Lett. **99**, 241103 (2007); P. Wolf *et al.*, Phys. Rev. Lett. **96**, 060801 (2006); H. Dehmelt *et al.*, Phys. Rev. Lett. **83**, 4694 (1999); B. Heckel *et al.*, Phys. Rev. Lett. **97**, 021603 (2006); M. D. Messier, in *Proceedings of the Third Meeting on CPT and Lorentz Symmetry*, edited by V. A. Kostelecký (World Scientific, Singapore, 2005), p. 84.

[6] P. Adamson *et al.*, Phys. Rev. D **77**, 072002 (2008).

[7] L. B. Auerbach *et al.*, Phys. Rev. D **72**, 076004 (2005).

[8] D. G. Michael *et al.*, Phys. Rev. Lett. **97**, 191801 (2006).

[9] O. W. Greenberg, Phys. Rev. Lett. **89**, 231602 (2002).

[10] H. Nunokawa, S. J. Parke, and R. Zukanovich Funchal, Phys. Rev. D **72**, 013009 (2005).

[11] D. G. Michael *et al.*, arXiv:0805.3170.

[12] N. Tagg *et al.*, Nucl. Instrum. Methods Phys. Res., Sect. A **539**, 668 (2005).

[13] P. Adamson *et al.* (to be published).

[14] P. Adamson *et al.*, Phys. Rev. D **76**, 072005 (2007).

[15] W. H. Press, B. Flannery, S. Teukolsky, and W. Vetterling, *Numerical Recipes in C* (Cambridge University Press, Cambridge, England, 1999).

[16] B. J. Rebel and S. L. Mufson, in *Proceedings of the Fourth Meeting on CPT and Lorentz Symmetry*, edited by V. A. Kostelecký (World Scientific, Singapore, 2008).